Study on Band Gaps of the Photonic Crystal in THz Frequency Range Based on the Periodic WCS-PSTD Method

Juan Chen, Anxue Zhang, and Jianjun Li

[1] The Key Laboratory for Physical Electronics and Devices of the Ministry of Education
Xi'an Jiaotong University, Xi'an, 710049, China
chen.juan.0201@mail.xjtu.edu.cn

Abstract ─ In this paper, a periodic weakly conditionally stable -pseudospectral time domain (WCS-PSTD) method is presented to simulate photonic crystal in Terahertz frequency range. The time step size in this method is only determined by the mesh length Δz and the spatial discretization along the z direction only needs two cells per minimum wavelength. The 3D formulas of the method are presented and the time stability condition of the method is demonstrated. Numerical results show that this method is more efficient than the periodic finite difference time domain (FDTD) method in terms of computer memory and computation time.

Index Terms ─ Finite difference time domain, pseudospectral method, time stability condition, weakly conditionally stable.

I. INTRODUCTION

Terahertz (THz) wave has significant transmission loss in free space, so the design and fabrication of controlling device for THz frequency radiation are imperative. Photonic crystal as a novel artificial material has photonic band gaps characteristic [1, 2]. It can be used to control the transmission of THz wave. Therefore, study on the photonic crystal has important effect on the development of Terahertz technique.

The finite-difference time-domain (FDTD) method is one of the most effective tools for the analysis of the photonic crystal [3, 4]. However, because the cross-section of the photonic crystal is circular, staircase approximation is used to model the curved surface. To decrease the approximation error, the cells' size must be very small compared with the wavelength. These fine cells reduce the time step size in the FDTD method, and hence, the FDTD method is computationally expensive. In addition, in the THz frequency region, the longitudinal direction of the photonic crystal is electrically large structure in most cases. Applying the FDTD method to simulate electrically large object, to decrease the dispersion error, a large number of cells (typically 10-20 cells per wavelength) are required. This stringent requirement severely limits the length of the photonic crystal solvable and increases the computation time inevitably.

Recently, a new weakly conditionally stable-pseudospectral time domain (WCS-PSTD) method [5] which is based on the hybrid implicit explicit difference technique [6-9] and the pseudospectral scheme [10-12] is presented. In this method, the time step size is not confined by fine cells and is extremely useful for problems with very fine structures along one or two directions. Meanwhile, this method allows a coarse spatial discretization that only needs two cells per minimum wavelength. Thus, for the simulation of the object which has fine and electrically large structures simultaneously, the WCS-PSTD algorithm is more efficient than the FDTD method in terms of computer memory and computation time. However, for the simulation of the photonic crystal which has periodic structures, the WCS-PSTD method needs to cope with the periodic boundary.

To solve this problem, this paper presents a periodic WCS-PSTD method which introduces the periodic boundary in the conventional WCS-PSTD method [5]. It also combines the hybrid implicit explicit difference technique with the pseudospectral scheme. The time step size in this method is not confined by fine cells and the space discretization along electrically large direction only needs two cells per minimum wavelength. The 3D formulas of the periodic WCS-PSTD method are presented, and final updating equations are given. The time stability condition and space discretization limitation of the method are discussed. When this method is applied to simulate photonic crystal, high computational efficiency is obtained and less computer memory is required, which is demonstrated through numerical examples by comparing with the periodic FDTD method.

By using the periodic WCS-PSTD method to simulate the photonic crystal, some useful conclusions are obtained. The simulation result shows that the photonic crystal has obvious band gap characteristic. The frequency and bandwidth of the band gap have relation with the permittivity of the photonic crystal. As the

Submitted On: June 19, 2014
Accepted On: June 11, 2015

increase of the permittivity, the frequency of the band gap decreases and the relative bandwidth of the band gap becomes wider. Besides, the smaller the radius and period length of the photonic crystal are, the higher the frequency range of the band gap. The relative bandwidth of the band gap reaches maximum value when the ratio between the diameter of the photonic crystal and the period length is 0.6.

II. FORMULATIONS

Figure 1 shows a schematic view of the photonic crystal under study. The cross-section of the photonic crystal is circular and needs to use very small cells to staircase approximation, as shown in Fig. 2. The length (L) of the photonic crystal is much larger than the wavelength in the THz frequency region. Typically, it is 20-30 times the wavelength. So, the photonic crystal is a complicated structure which has fine size (along the x and y direction) and electrically large size (along the z direction) simultaneously.

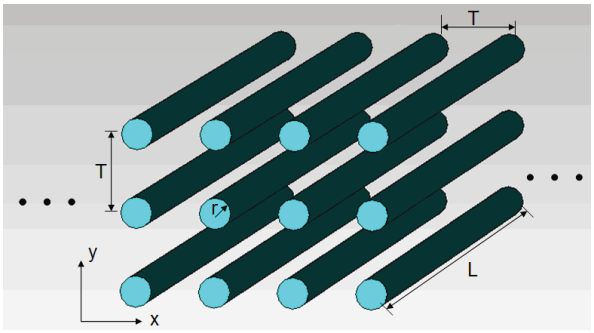

Fig. 1. Schematic view of photonic crystal.

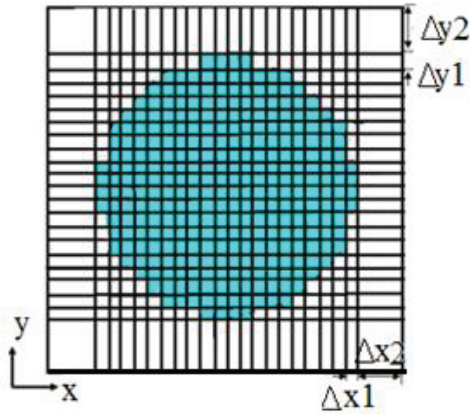

Fig. 2. The staircase approximation of the photonic crystal's cross-section.

In the FDTD method, the small cell sizes $\Delta x1$ and $\Delta y1$ will confine the time step size Δt and result in a large number of computation time. To remove the confine of the fine space increment on the time step size, the periodic WCS-PSTD method uses a hybrid implicit explicit difference technique to replace the explicit difference along the x and y directions. The 3D formulas for the periodic WCS-PSTD method are as follows:

<First procedure>

$$\varepsilon\frac{E_x^{n+1/2}-E_x^n}{\Delta t}=\frac{\partial\left(H_z^{n+1/2}+H_z^n\right)}{2\partial y}-\frac{\partial H_y^n}{\partial z}, \tag{1.1}$$

$$E_y^{n+1/2}=E_y^n, \tag{1.2}$$

$$\varepsilon\frac{E_z^{n+1/2}-E_z^n}{\Delta t}=\frac{\partial\left(H_y^{n+1/2}+H_y^n\right)}{2\partial x}, \tag{1.3}$$

$$H_x^{n+1/2}=H_x^n, \tag{1.4}$$

$$\mu\frac{H_y^{n+1/2}-H_y^n}{\Delta t}=\frac{\partial\left(E_z^{n+1/2}+E_z^n\right)}{2\partial x}-\frac{\partial E_x^{n+1/2}}{\partial z}, \tag{1.5}$$

$$\mu\frac{H_z^{n+1/2}-H_z^n}{\Delta t}=\frac{\partial\left(E_x^{n+1/2}+E_x^n\right)}{2\partial y}. \tag{1.6}$$

<Second procedure>

$$E_x^{n+1}=E_x^{n+1/2}, \tag{2.1}$$

$$\varepsilon\frac{E_y^{n+1}-E_y^{n+1/2}}{\Delta t}=\frac{\partial H_x^{n+1/2}}{\partial z}-\frac{\partial\left(H_z^{n+1/2}+H_z^{n+1}\right)}{2\partial x}, \tag{2.2}$$

$$\varepsilon\frac{E_z^{n+1}-E_z^{n+1/2}}{\Delta t}=-\frac{\partial\left(H_x^{n+1/2}+H_x^{n+1}\right)}{2\partial y}, \tag{2.3}$$

$$\mu\frac{H_x^{n+1}-H_x^{n+1/2}}{\Delta t}=\frac{\partial E_y^{n+1}}{\partial z}-\frac{\partial\left(E_z^{n+1/2}+E_z^{n+1}\right)}{2\partial y}, \tag{2.4}$$

$$H_y^{n+1}=H_y^{n+1/2}, \tag{2.5}$$

$$\mu\frac{H_z^{n+1}-H_z^{n+1/2}}{\Delta t}=-\frac{\partial\left(E_y^{n+1/2}+E_y^{n+1}\right)}{2\partial x}, \tag{2.6}$$

where n and Δt are the index and size of time step.

The calculation for one discrete time step is performed using two procedures in the periodic WCS-PSTD method. The first procedure is based on Eqs. (1.1)-(1.6), and the second procedure is based on Eqs. (2.1)-(2.6). It can be seen from these equations that for the spatial derivatives ∂x and ∂y, a hybrid implicit explicit difference technique is used; thus, the equations (1.1), (1.3), (1.5), (1.6), (2.2)-(2.4) and (2.6) can't be calculated directly, because they all include the unknown components defined at the same time step. For example, updating of $E_x^{n+1/2}$ component, as shown in Eq. (1.1), needs the unknown $H_z^{n+1/2}$ components at the same time step; thus the $E_x^{n+1/2}$ component has to be updated implicitly. By substituting Eq. (1.6) into Eq. (1.1), the equation for $E_x^{n+1/2}$ component is given as:

$$\left(1-\frac{\Delta t^2}{4\varepsilon\mu}\frac{\partial^2}{\partial^2 y}\right)E_x^{n+1/2} = \left(1+\frac{\Delta t^2}{4\varepsilon\mu}\frac{\partial^2}{\partial^2 y}\right)E_x^n - \frac{\Delta t}{\varepsilon}\frac{\partial H_y^n}{\partial z}+\frac{\Delta t}{\varepsilon}\frac{\partial H_z^n}{\partial y}. \tag{3}$$

Because the periodic WCS-PSTD method applies the hybrid implicit explicit difference technique to the derivatives ∂x and ∂y, its time step size will have no relation with the spatial increments Δx and Δy. This will be demonstrated in the next section.

In the FDTD method, to decrease the dispersion error resulted from the spatial finite difference, spatial discretization should satisfy the condition that 10-20 cells per wavelength are required. This stringent requirement causes a large number of cells along the z direction in the simulation of the photonic crystal, because the longitudinal direction of the photonic crystal is often larger than the wavelength. It not only severely increases the memory requirement, but also increases the computation time.

To overcome the limit of the wavelength on the space discretization Δz, the periodic WCS-PSTD method uses a Fourier transform algorithm instead of finite difference to represent the spatial derivative ∂z. This allows a coarse spatial discretization along z direction that only two nodes per minimum wavelength are required (the demonstration will be shown in the next section). For other spatial derivatives ∂x and ∂y, it also applies centered second-order finite differences as that in the standard FDTD method. Thus, the equation for $E_x^{n+1/2}$ component can be obtained as follows:

$$\begin{aligned}&\left(1+2\tau_1\right)E_x^{n+1/2}\left(i+1/2,j,k\right)-\tau_1 E_x^{n+1/2}\left(i+1/2,j+1,k\right)\\&-\tau_1 E_x^{n+1/2}\left(i+1/2,j-1,k\right)\\&=\left(1-2\tau_1\right)E_x^{n}\left(i+1/2,j,k\right)+\tau_1 E_x^{n}\left(i+1/2,j+1,k\right)\\&+\tau_1 E_x^{n}\left(i+1/2,j-1,k\right)\\&+\frac{\Delta t}{\varepsilon\Delta y}\left[H_z^n\left(i+1/2,j+1/2,k\right)-H_z^n\left(i+1/2,j-1/2,k\right)\right]\\&-\frac{\Delta t}{\varepsilon}\Im^{-1}\left\{\hat{j}k_z\Im\left[H_y^n\left(i+1/2,j,k\right)\right]\right\},\end{aligned} \tag{4}$$

where, $\hat{j}=\sqrt{-1}$, $\tau_1=\Delta t^2/4\varepsilon\mu\Delta y^2$, Δy is the spatial increment along y direction; *i*, *j*, and *k* denote the indices of spatial increments respectively along x, y, and z directions; $\Im$ and $\Im^{-1}$ represent the Fourier transforms and inverse Fourier transforms which were described in detail in references [13].

After $E_x^{n+1/2}$ component is obtained by using equation (4), component $H_z^{n+1/2}$ is explicitly updated straightforward as follows:

$$\begin{aligned}&H_z^{n+1/2}\left(i+1/2,j+1/2,k\right)=H_z^{n}\left(i+1/2,j+1/2,k\right)\\&+\frac{\Delta t}{2\mu\Delta y}\left[\begin{aligned}&E_x^{n+1/2}\left(i+1/2,j+1,k\right)-E_x^{n+1/2}\left(i+1/2,j,k\right)\\&+E_x^{n}\left(i+1/2,j+1,k\right)-E_x^{n}\left(i+1/2,j,k\right)\end{aligned}\right].\end{aligned} \tag{5}$$

By following the same procedure, the equation for $E_z^{n+1/2}$ component can be obtained as follows:

$$\begin{aligned}&\left(1+2\tau_2\right)E_z^{n+1/2}\left(i,j,k+1/2\right)-\tau_2 E_z^{n+1/2}\left(i+1,j,k+1/2\right)\\&-\tau_2 E_z^{n+1/2}\left(i-1,j,k+1/2\right)\\&=\left(1-2\tau_2\right)E_z^{n}\left(i,j,k+1/2\right)+\tau_2 E_z^{n}\left(i+1,j,k+1/2\right)\\&+\tau_2 E_z^{n}\left(i-1,j,k+1/2\right)\\&+\frac{\Delta t}{\varepsilon\Delta x}\left[H_y^n\left(i+1/2,j,k\right)-H_y^n\left(i-1/2,j,k\right)\right]\\&-\frac{\Delta t^2}{2\varepsilon\mu\Delta x}\Im^{-1}\left\{\hat{j}k_z\Im\left[E_x^{n+1/2}\left(i+1/2,j,k\right)\right]\right\}\\&+\frac{\Delta t^2}{2\varepsilon\mu\Delta x}\Im^{-1}\left\{\hat{j}k_z\Im\left[E_x^{n+1/2}\left(i-1/2,j,k\right)\right]\right\},\end{aligned} \tag{6}$$

where, $\tau_2=\Delta t^2/4\varepsilon\mu\Delta x^2$, Δx is the spatial increment along x direction.

Because the photonic crystal has periodic structure along the x direction, the computation of $E_z^{n+1/2}$ component at the periodic boundary needs to be modified as follows:

$$\begin{aligned}&E_z^{n+1/2}\left(i,j,k+1/2\right)\\&-\tau_2\left[E_z^{n+1/2}\left(2,j,k+1/2\right)-E_z^{n+1/2}\left(1,j,k+1/2\right)\right]\\&+\tau_2\left[E_z^{n+1/2}\left(I,j,k+1/2\right)-E_z^{n+1/2}\left(I-1,j,k+1/2\right)\right]\\&=E_z^{n}\left(i,j,k+1/2\right)\\&+\tau_2\left[E_z^{n}\left(2,j,k+1/2\right)-E_z^{n}\left(1,j,k+1/2\right)\right]\\&-\tau_2\left[E_z^{n}\left(I,j,k+1/2\right)-E_z^{n}\left(I-1,j,k+1/2\right)\right]\\&+\frac{\Delta t}{\varepsilon\Delta x}\left[H_y^n\left(1+1/2,j,k\right)-H_y^n\left(I-1/2,j,k\right)\right]\\&-\frac{\Delta t^2}{2\varepsilon\mu\Delta x}\Im^{-1}\left\{\hat{j}k_z\Im\left[E_x^{n+1/2}\left(1+1/2,j,k\right)\right]\right\}\\&+\frac{\Delta t^2}{2\varepsilon\mu\Delta x}\Im^{-1}\left\{\hat{j}k_z\Im\left[E_x^{n+1/2}\left(I-1/2,j,k\right)\right]\right\},\end{aligned} \tag{7}$$

here, $i=1$ and I denote the meshes at the periodic boundary respectively.

The computations for other components $H_y^{n+1/2}$, E_y^{n+1}, E_z^{n+1}, H_x^{n+1} and H_z^{n+1} can be obtained by following the same procedure and will not be discussed in detail.

It should be noted that, in contrast to the standard Yee's algorithm, the periodic WCS-PSTD method does not require a spatially staggered grid along the z direction, because Fourier transforms operation is

global. It means that the field components E_x and H_y, E_y and H_x are located at the same nodes in the periodic WCS-PSTD method, as shown in Fig. 3.

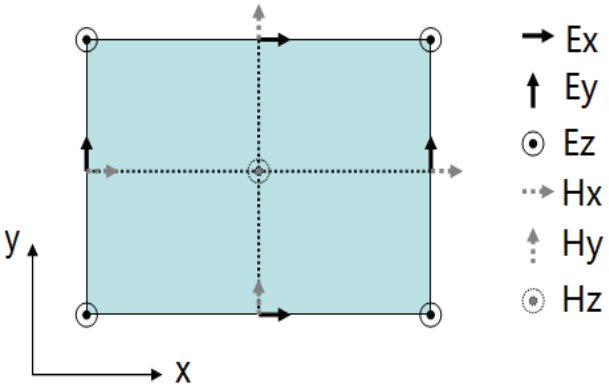

Fig. 3. Spatial grid of the field components in the periodic WCS-PSTD method.

III. STABILITY AND NUMERICAL DISPERSION ANALYSIS

The relations between field components of Eqs. (1) and (2) can be represented in a matrix form as follows:

$$[E]U^{n+1/2} = [F]U^{n}, \tag{8}$$

$$[C]U^{n+1} = [D]U^{n+1/2}, \tag{9}$$

where,

$$[E] = \begin{bmatrix} 1 & 0 & 0 & 0 & 0 & -aD_y/2 \\ 0 & 1 & 0 & 0 & 0 & 0 \\ 0 & 0 & 1 & 0 & -aD_x/2 & 0 \\ 0 & 0 & 0 & 1 & 0 & 0 \\ bD_z & 0 & -bD_x/2 & 0 & 1 & 0 \\ -bD_y/2 & 0 & 0 & 0 & 0 & 1 \end{bmatrix},$$

$$[F] = \begin{bmatrix} 1 & 0 & 0 & 0 & -aD_z & aD_y/2 \\ 0 & 1 & 0 & 0 & 0 & 0 \\ 0 & 0 & 1 & 0 & aD_x/2 & 0 \\ 0 & 0 & 0 & 1 & 0 & 0 \\ 0 & 0 & bD_x/2 & 0 & 1 & 0 \\ bD_y/2 & 0 & 0 & 0 & 0 & 1 \end{bmatrix},$$

$$[C] = \begin{bmatrix} 1 & 0 & 0 & 0 & 0 & 0 \\ 0 & 1 & 0 & 0 & 0 & aD_x/2 \\ 0 & 0 & 1 & aD_y/2 & 0 & 0 \\ 0 & -bD_z & bD_y/2 & 1 & 0 & 0 \\ 0 & 0 & 0 & 0 & 1 & 0 \\ 0 & bD_x/2 & 0 & 0 & 0 & 1 \end{bmatrix},$$

$$[D] = \begin{bmatrix} 1 & 0 & 0 & 0 & 0 & 0 \\ 0 & 1 & 0 & aD_z & 0 & -aD_x/2 \\ 0 & 0 & 1 & -aD_y/2 & 0 & 0 \\ 0 & 0 & -bD_y/2 & 1 & 0 & 0 \\ 0 & 0 & 0 & 0 & 1 & 0 \\ 0 & -bD_x/2 & 0 & 0 & 0 & 1 \end{bmatrix},$$

$U^n = \begin{bmatrix} E_x^n & E_y^n & E_z^n & H_x^n & H_y^n & H_z^n \end{bmatrix}^t$, $a = \Delta t/\varepsilon$, $b = \Delta t/\mu$, $D_m = \partial/\partial m$ ($m = x, y, z$) represents the first derivative operator with respect to m.

By substituting Eq. (9) into Eq. (8), it obtains:

$$\left([E][C]\zeta - [E][D][E]^{-1}[F]\right)U^n = 0, \tag{10}$$

ζ indicates growth factor. By applying the forward Fourier transforms to both sides of equation (10), it obtains equation (11), where, $X = \dfrac{abD_x^2}{4}$, $Z = \dfrac{ab(jk_z)^2}{4}$, $Y = \dfrac{abD_y^2}{4}$, $S = (1-X)(1-Y)$, $T = \dfrac{abD_xD_y}{4}$:

$$\begin{bmatrix} \zeta-1 & -T(\zeta+1) & 0 & 0 & aD_z & -\dfrac{aD_y}{2}(\zeta+1) \\ \dfrac{2T}{(1-Y)} & \zeta-1 & 0 & -aD_z & \dfrac{-aD_zT}{(1-Y)} & \dfrac{aD_x}{2}\left(\zeta+\dfrac{1+Y}{1-Y}\right) \\ 0 & 0 & \zeta-1 & \dfrac{aD_y}{2}(\zeta+1) & \dfrac{-aD_x(\zeta+1)}{2} & 0 \\ \dfrac{-bD_zT(1+Y)}{S} & -b\zeta D_z & \dfrac{bD_y}{2}\left(\zeta+\dfrac{(1+X)}{(1-X)}\right) & \zeta-1 & \dfrac{2T(1-Y+2Z)}{S} & \dfrac{-abD_xD_zY}{S} \\ b\zeta D_z & 0 & \dfrac{-bD_x}{2}(\zeta+1) & -T(\zeta+1) & \zeta-1 & 0 \\ \dfrac{-bD_y}{2}(\zeta+1) & \dfrac{bD_x}{2}(\zeta+1) & 0 & 0 & 0 & \zeta-1 \end{bmatrix} U^n = 0. \tag{11}$$

For a nontrivial solution of (11), the determinant of the coefficient matrix in (11) should be zero. It can be obtained:

$$(\zeta-1)^2\left[\begin{matrix}(\zeta-1)^2-4Z\zeta-Y(\zeta+1)^2\\-X(\zeta+1)^2+XY(\zeta+1)^2\end{matrix}\right]^2=0. \quad (12)$$

By solving equation (12), the growth factor ζ is obtained:

$$\zeta_1=1, \quad (13)$$

$$\zeta_{2,3}=\frac{N\pm\sqrt{N^2-R^2}}{R}, \quad (14)$$

where, $R=1-X-Y+XY$, $N=1+X+Y+2Z-XY$. According to the stability condition during field advancement, the module of growth factor ζ cannot be larger than 1. In equation (14), the relation $|\zeta_{2,3}=1|$ can be obtained when the condition $R^2\geq N^2$ is satisfied. D_x and D_y represent the first derivative operator with respect to x and y. They are approximated by centered second-order finite differences. So it has the relations $D_x=2j\sin(k_x\Delta x/2)/\Delta x$ and $D_y=2j\sin(k_y\Delta y/2)/\Delta y$ [6],

$$R^2\geq N^2\Rightarrow 1+Z\geq 0. \quad (15)$$

Because the maximum value of k_z is $\frac{2\pi}{2\Delta z}$, it has:

$$ab\left(\frac{2\pi}{2\Delta z}\right)^2\leq 4\Rightarrow\Delta t\leq\frac{2\Delta z}{c\pi}, \quad (16)$$

where, $c=1/\sqrt{\varepsilon\mu}$ is the speed of light in the medium.

It can be seen from Eq. (16) that the maximum time step size in the periodic WCS-PSTD method is only determined by the cell size Δz. This is very useful when the object of analysis has fine scale dimensions along the x and y directions.

By substituting the expression $\zeta=e^{j\omega\Delta t}$ into equation (12), the dispersion relation for the periodic WCS-PSTD method can be obtained as follows:

$$\sin^2\left(\frac{\omega\Delta t}{2}\right)=\frac{r_y^2+r_x^2+r_z^2+r_x^2r_y^2}{1+r_x^2+r_y^2+r_x^2r_y^2}, \quad (17)$$

where, $r_z=(c\Delta t k_z/2)^2$, $r_x=\left(c\Delta t\sin(k_x\Delta x/2)/\Delta x\right)^2$, $r_y=\left(c\Delta t\sin(k_y\Delta y/2)/\Delta y\right)^2$. It can be seen from equation (17) that the numerical dispersion error of the periodic WCS-PSTD method has no relation with the spatial cell size Δz. It is only decided by the cell sizes Δx, Δy, and the time step size Δt. As a result, the spatial cell size Δz is not confined by the wavelength. It only needs to satisfy the Nyquist sampling theorem that only two nodes per minimum wavelength are required along the z direction.

It concludes from above analysis that in the periodic WCS-PSTD method, the time step size Δt is only determined by the spatial increment Δz, and spatial increment Δz only needs to satisfy with the condition: $\Delta z\leq\lambda_{\text{minimum}}/2$. This will be very useful in the simulation of the photonic crystal, because the photonic crystal has very fine scale along x and y directions and is electrically large along z direction. For solving this problem the periodic WCS-PSTD method is more efficient than the periodic FDTD method in terms of computer memory and computation time, which will be demonstrated in next section.

IV. SIMULATION AND ANALYSIS

To demonstrate the accuracy and efficiency of the periodic WCS-PSTD method, the photonic crystal shown in Fig. 1 is simulated. The radius (r) and length (L) of the photonic crystal are 20 um and 3000 um, respectively. The period length of the photonic crystal is T=100 um. The material of the photonic crystal is silicon with dielectric constant $\varepsilon_r=11.7$. A uniform plane wave polarized along the x direction is normally incident on the photonic crystal. The propagation direction of the wave is along the y direction. The time dependence of the excitation function is as follows:

$$E_x(t)=\exp[-\frac{4\pi(t-t_0)^2}{t_1^2}], \quad (18)$$

where, t_0 and t_1 are constants, and both equal to 1×10^{-12}s. In such a case, the highest frequency of interest is 2 THz and the minimum wavelength of the source is about 150 um.

The periodic WCS-PSTD method is used to simulate the transmitted field at the back of the photonic crystal. For comparison, the results calculated by the periodic FDTD method are also shown. Because the structure has circular cross-section, it is discretized by using staircase approximation, as shown in Fig. 2. To guarantee the computational accuracy, the circle is discretized by using 20×20 cells, so the cell sizes $\Delta x1$ and $\Delta y1$ are both equal to 2 um, corresponding to 1/75 of the minimum wavelength. In other computation domain, $\Delta x2$ and $\Delta y2$ are 3 um and 15 um, respectively. Along the z direction, for the periodic FDTD method, considering the limit of the wavelength on the space discretization, the space increment Δz is selected to be 15 um, corresponding to 1/10 of the minimum wavelength. While for the periodic WCS-PSTD method, space increment Δz can be increased to 75 um, corresponding to 1/2 of the minimum wavelength. To cut off the outer boundary, periodic boundary condition is applied along the x direction and convolutional perfectly matched layer (CPML) that are ten cells thick are applied along the y and z directions. Thus, for the periodic FDTD

and periodic WCS-PSTD methods, the total mesh numbers are 40×110×240 and 40×110×80, respectively. The time step size in the periodic FDTD method is:

$$\Delta t = 1\Big/ c\sqrt{\left(\frac{1}{2\times10^{-6}}\right)^2+\left(\frac{1}{2\times10^{-6}}\right)^2+\left(\frac{1}{15\times10^{-6}}\right)^2} = 4.69\times10^{-3}\,\text{ps},$$

which is the maximum time step size to ensure the numerical stability. In the periodic WCS-PSTD method, the time step size that is only determined by cell size Δz is selected to be $\Delta t = \dfrac{2\times75\times10^{-6}}{c\pi} = 159\times10^{-3}$ ps, which is 34 times as that of the periodic FDTD method.

Figure 4 depicts the transmitted field E_x calculated by using the periodic FDTD method and the periodic WCS-PSTD method. It can be seen from this figure that the results of these two methods agree very well with each other, which shows the periodic WCS-PSTD method has high computational accuracy.

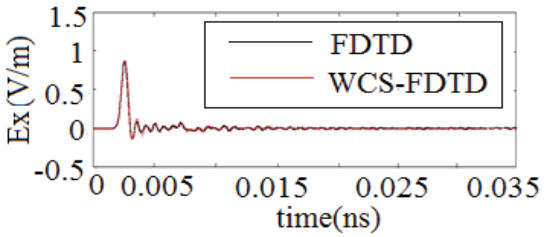

Fig. 4. The transmitted field E_x calculated by using periodic FDTD method and periodic WCS-PSTD method.

The computation time and memory requirement of the simulation above are summarized in Table 1. It can be seen from this table that both the memory requirement and computation time of the periodic WCS-PSTD method are reduced significantly compared with those of the periodic FDTD method. Because large spatial cell and large time step size are used, the memory requirement of the periodic WCS-PSTD method is reduced by 60%, and its computation time is almost 1/30 of that of the periodic FDTD method.

Table 1: Simulation time and memory requirement for the periodic FDTD method and periodic WCS-PSTD method

	Δz (um)	Δt (ps)	Time (minute)	Memory Requirement (Mb)
FDTD method	15	0.0046	320	311.73
WCS-PSTD method	75	0.159	12	115.45

The transmission coefficient (Tr) of the photonic crystal calculated by using the periodic FDTD method and the periodic WCS-PSTD method are presented in Fig. 5. The computation formula of Tr is as follows:

$$T_r = 20\log_{10}\left|E_x/E_x^{'}\right|, \tag{19}$$

here, E_x denotes the transmitted field E_x calculated by using the periodic FDTD method and the periodic WCS-PSTD method; $E_x^{'}$ is the magnitude of the incident wave.

It can be seen from Fig. 5 that in the frequency range from 1.5 THz to 1.8 THz, the transmission coefficient Tr is below to -10 dB. This is a direct evidence of that the photonic crystal has obvious band gap in this frequency range. The relative bandwidth of the band gap is 18.18%. The distribution of the electric field E_x at frequency 1.7 THz is shown in Fig. 6. From this figure, it can be seen that the incident wave is reflected completely and little wave penetrates the photonic crystal at this frequency.

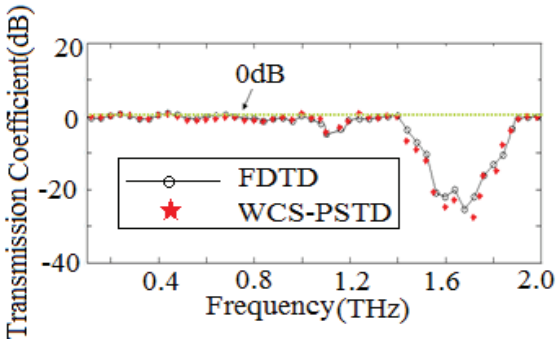

Fig. 5. The transmission coefficient of the photonic crystal calculated by using the periodic FDTD method and the periodic WCS-PSTD method.

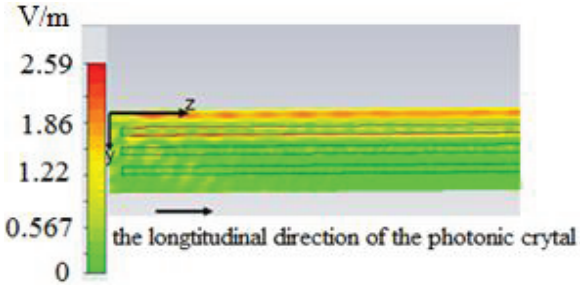

Fig. 6. The distribution of the electric field E_x at frequency 1.7 THz.

It should be noted that in Fig. 5 there is a slightly divergence between the results of the periodic FDTD method and the periodic WCS-PSTD method at 1.7 THz. The difference between these two methods in time domain is too small to be neglected, as shown in Fig. 4, but in frequency domain, it is enlarged by the resonance effect of the photonic crystal at 1.7 THz. The divergence between these two methods is brought about by the

splitting-error in the periodic WCS-PSTD method. The periodic WCS-PSTD method applies the hybrid implicit explicit difference technique. This technique will bring a splitting error which is proportional to the time step size. The detailed discussion about the splitting error of the hybrid implicit explicit difference technique has been presented in [14]. So, compared with the periodic FDTD method, the accuracy of the WCS-PSTD is reduced slightly. However, this reduction of the accuracy doesn't affect the periodic WCS-PSTD method to get correct results. The periodic WCS-PSTD method can be used in the analysis which doesn't require the accuracy strictly.

Because the periodic WCS-PSTD method is more efficient than the periodic FDTD method in terms of computer memory and computational time, it is used to analyze the band gap characteristic of the photonic crystal in detail.

Firstly, the relation between the frequency range of band gap and the radius of the photonic crystal is analyzed. The length and period of the photonic crystal is 3000 um and 100 um. The radius of the photonic crystal increases from 5 um to 40 um. The variations of the frequency range of the band gap with respect to radius are shown in Table 2. In this table, Rt which is equal to $2\times r/T$ represents the ratio between the diameter of the photonic crystal and the period length. It can be seen from this table that as the increase of the radius, the band gap of the photonic crystal moves to a lower frequency range. The relative bandwidth of the band gap has maximum value equal to 29.85% when the radius of the photonic crystal is 30 um.

Table 2: Variations of the frequency range of the band gap with respect to the radius

r (um)	Rt	Frequency Range (THz)	Relative Bandwidth
10	0.2	2.70-2.80	3.64%
15	0.3	1.97-2.06	4.47%
20	0.4	1.50-1.80	18.18%
25	0.5	1.30-1.75	29.51%
30	0.6	1.14-1.54	29.85%
35	0.7	1.03-1.33	25.42%
40	0.8	0.97-1.18	19.53%

When it keeps the radius r=20 um unchanged and increases the period length of the photonic crystal from 50 um to 200 um, the band gap of the photonic crystal also moves to a lower frequency range, as shown in Table 3. The relative bandwidth of the band gap has maximum value equal to 30.12% when period length of the photonic crystal is 66.66 um.

From Table 2 and 3, we can see that the relative bandwidth of the band gap is mainly determined by the ratio between the diameter and the period length. It reaches its maximum value when the ratio is 0.6, no matter what the radius and period length are.

Table 3: Variations of the frequency range of the band gap with respect to the period length

T (um)	Rt	Frequency Range (THz)	Relative Bandwidth
50	0.8	1.94-2.37	19.95%
60	0.7	1.78-2.32	26.34%
66.66	0.6	1.72-2.33	30.12%
80	0.5	1.62-2.19	29.92%
100	0.4	1.50-1.80	18.18%
133	0.3	1.48-1.61	4.85%
200	0.2	1.34-1.37	3.97%

In addition, the frequency range and relative bandwidth of the band gap also have relation with the dielectric constant of the photonic crystal. The variations of the frequency range and bandwidth with respect to relative dielectric constant ε_r are shown in Table 4. Here, the geometry of the photonic crystal, including the period length, radius and length, are unchanged. It can be seen from this table that as the increase of the dielectric constant, the frequency of the band gap decreases and the relative bandwidth becomes wider.

However, if the polarization of the incident wave is along the z direction, namely, the longitudinal direction of the photonic crystal, the band gap characteristic will become unobvious. The transmission coefficient of the photonic crystal impinged by a plane wave polarized along the z direction is shown in Fig. 7. In this figure, the transmission coefficient is above -10 dB in all the frequency range, which means that some incident wave passes through the photonic crystal and the band gap of the photonic crystal disappears.

Table 4: Variations of the frequency range of the band gap with respect to relative dielectric constant

ε_r	Frequency Range (THz)	Relative Bandwidth
3	2.64-2.67	1.13%
5	2.23-2.67	7.34%
7	1.94-2.16	10.73%
9	1.74-2.01	14.40%
11	1.60-1.90	17.14%
13	1.48-1.83	21.25%

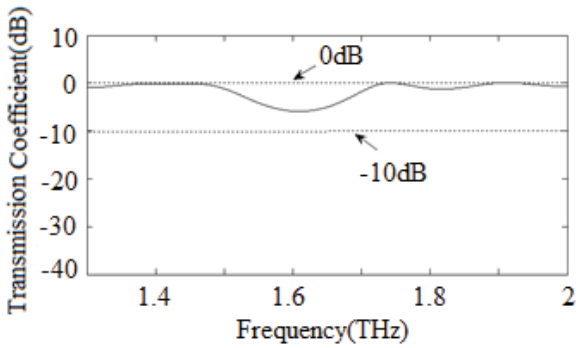

Fig. 7. The transmission coefficient of the photonic crystal impinged by a plane wave polarized along the z direction.

To validate this, the distribution of the electric field E_z at the frequency 1.7 THz is depicted in Fig. 8. It can be seen from this figure, that at this case most of the incident wave penetrate the photonic crystal obviously.

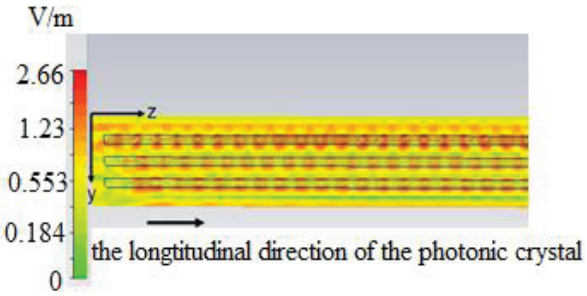

Fig. 8. The distribution of the electric field E_z at frequency 1.7 THz.

It concludes from the analysis above that when the photonic crystal is impinged by a plane wave polarized along the radial direction, the photonic crystal exhibits obvious band gap characteristic; the smaller the radius and period length of the photonic crystal are, the higher the frequency range of the band gap. The relative bandwidth of the band gap reaches maximum value when the ratio between the diameter of the photonic crystal and the period length is 0.6. Besides, the frequency and bandwidth of the band gap have relation with the permittivity. As the increase of the permittivity, the frequency of the band gap decreases and the relative bandwidth of the band gap becomes wider.

VI. CONCLUSION

This paper introduces a periodic WCS-PSTD method which is based on the hybrid implicit explicit difference technique and pseudospectral scheme to simulate the photonic crystal. The maximum time step size in this method is only determined by cell size Δz and the spatial discretization along z direction only needs two cells per wavelength. When this method is applied to simulate the photonic crystal, high computational efficiency is obtained and less computer memory is required, which is demonstrated through numerical examples by comparing with the periodic FDTD method. This method not only can be used in the simulation of photonic crystal, but also be useful in other electromagnetic problems where both fine and electrically large structures are used.

ACKNOWLEDGMENT

This work was supported by National Natural Science Foundations of China (No. 61001039 and 61231003), and also supported by the Fundamental Research Funds for the Central Universities.

REFERENCES

[1] S. Savel'ev, A. L. Rakhmanov, and F. Nori, "Using Josephson vortex lattices to control terahertz radiation: tunable transparency and terahertz photonic crystals," *Phys. Rev. Lett.*, vol. 94, no. 15, 157004, Apr. 2005.

[2] A. Bingham, Y. G. Zhao, and D. Grischkowsky, "THz parallel plate photonic waveguide," *Appl. Phys. Lett.*, vol. 87, no. 5, 051101, 2005.

[3] K. S. Yee, "Numerical solution of initial boundary value problems involving Maxwell's equations in isotropic media," *IEEE Trans. Antennas Propagat.*, vol. 14, no. 3, pp. 302-307, May 1966.

[4] A. Taflove, *Computational Electrodynamics*, Norwood, MA: Artech House, 1995.

[5] J. Chen and J. Wang, "The WCS-PSTD method for solving electromagnetic problems both with fine and electrically large structures," *IEEE Trans. Antennas Propagat*., vol. 62, no. 5, pp. 2695-2701, May 2014.

[6] J. Chen and J. Wang, "A novel WCS-FDTD method with weakly conditional stability," *IEEE Trans. Electromagn. Compat*., vol. 49, no. 2, pp. 419-426, Feb. 2007.

[7] J. Chen and C. M. Tian, "Using WCS-FDTD method to simulate various cylindrical metallic enclosures," *International Journal of Numerical Modelling: Electronic Networks, Devices and Fields*, vol. 24, no. 1, pp. 87-98, Jan. 2011.

[8] B. K. Huang, G. Wang, Y. S. Jiang, and W. B. Wang, "A hybrid implicit-explicit FDTD scheme with weakly conditional stability," *Microw. Opt. Tech. Letters*, vol. 39, no. 10, pp. 97-101, Oct. 2003.

[9] J. Chen and J. Wang, "A 3-D hybrid implicit-explicit FDTD scheme with weakly conditional stability," *Microwave Opt. Tech. Lett*., vol. 48, no. 11, pp. 2291-2294, Nov. 2006.

[10] Q. H. Liu, "Large-scale simulations of electromagnetic and acoustic measurements using the pseudospectral time-domain (PSTD) algorithm," *IEEE Trans. Geoscience and Remote Sensing*, vol. 37, no. 2, pp. 917-926, Mar. 1999.

[11] Q. L. Li and Y. C. Chen, "Application of the PSTD for scattering analysis," *IEEE Trans. Antennas Propagat.*, vol. 50, no. 9, pp. 1317-1319, Sep. 2002.

[12] Z. Lin, "The optimal spatially-smoothed source patterns for the pseudospectral time-domain method," *IEEE Trans. Antennas Propagat*., vol. 58, no. 1, pp. 227-229, Jan. 2010.

[13] W. H. Press, B. P. Flannery, S. A. Teukolsky, and W. T. Vetterling, *Numerical Recipes-The Art of Scientific Computing*, Cambridge: Cambridge University Press, 1986.

[14] J. Chen and J. G. Wang, "Weakly conditionally stable and unconditionally stable FDTD schemes for 3D Maxwell's equations," *Progr. Electromagn. Res. B*, vol. 19, pp. 329-366, 2010.

Juan Chen received the Ph.D. degree in Electromagnetic Field and Microwave Techniques at the Xi'an Jiaotong University, Xi'an, China, in 2008. She now serves as an Associate Professor at Xi'an Jiaotong University. Her research interests are the numerical electromagnetic methods, antenna designs, and electromagnetic compatibility.